

# MEMSENSE



## 1.0 Introduction

Inertial measurement units (IMUs) are used in a variety of applications. IMUs function by measuring the acceleration, angular velocity and in some cases magnetic field using accelerometers, gyroscopes and magnetometers. The sensor measurements encoded are communicated to a system to follow and control an object's position using a method known as dead reckoning.

In the modern inertial measurement unit (IMU) marketplace there is a wide variety of IMU choices from low cost to ultra high performance. Many customers ask "What's the difference between the low cost and the rest of the IMUs available?" There are many differences however one predominant difference is the vibration susceptibility of the sensors used in the low cost IMUs, namely the MEMS gyroscopes.

MEMSsense produced this report to depict the difference that vibration performance can make in dynamic applications. MEMSsense conducted performance testing of low cost triaxial MEMS gyroscopes under a range of random vibration amplitudes to determine this class of product's usefulness in vibratory environments.

IMUs containing low cost triaxial gyroscopes were subject to random vibration profiles over a range of acceleration levels. The aim of the study was to detect detrimental effects in the low cost triaxial MEMS gyroscopes that are utilized in low cost IMUs. These results were compared to MEMS gyro technologies that are utilized in the standard MEMSsense product line.

## Test Setup

A MEMSense IMU was chosen that is utilized in a highly dynamic missile environment that is configured to 5000 °/s, 600 °/s and 600 °/s in the gyro X, Y, and Z axes respectively. The same IMU was redesigned utilizing the latest low cost MEMS gyroscope technology configured to 6000 °/s, 500 °/s, and 500 °/s for the X, Y, and Z gyro axis respectively.

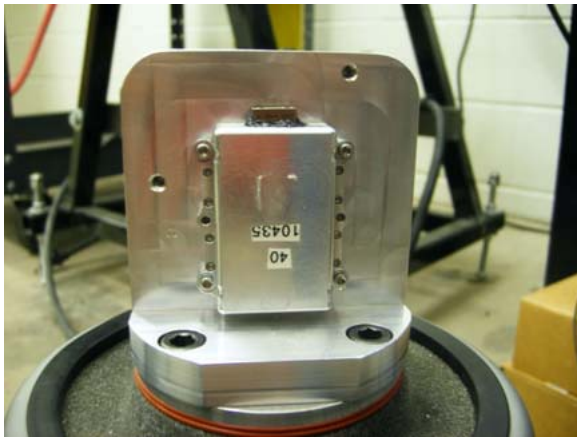


Figure 1: X Axis Test Configuration

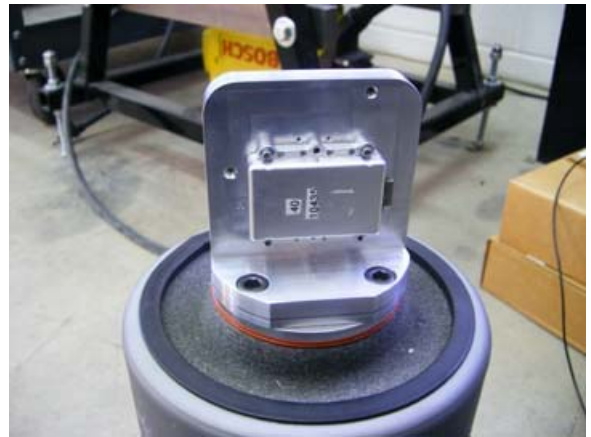


Figure 2: Y Axis Test Configuration

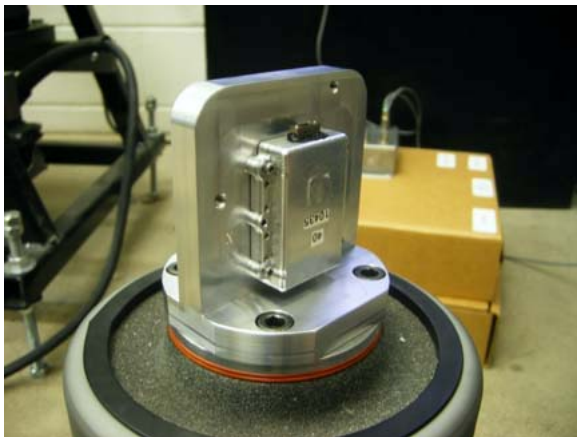


Figure 3: X Axis Test Configuration

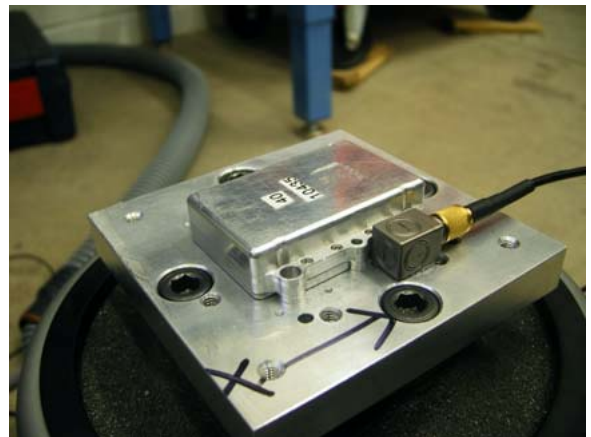


Figure 4: Z Axis Test Configuration

## 2.0 VIBRATION TESTING SPECIFICATION

### 2.1 Random Vibration Specification

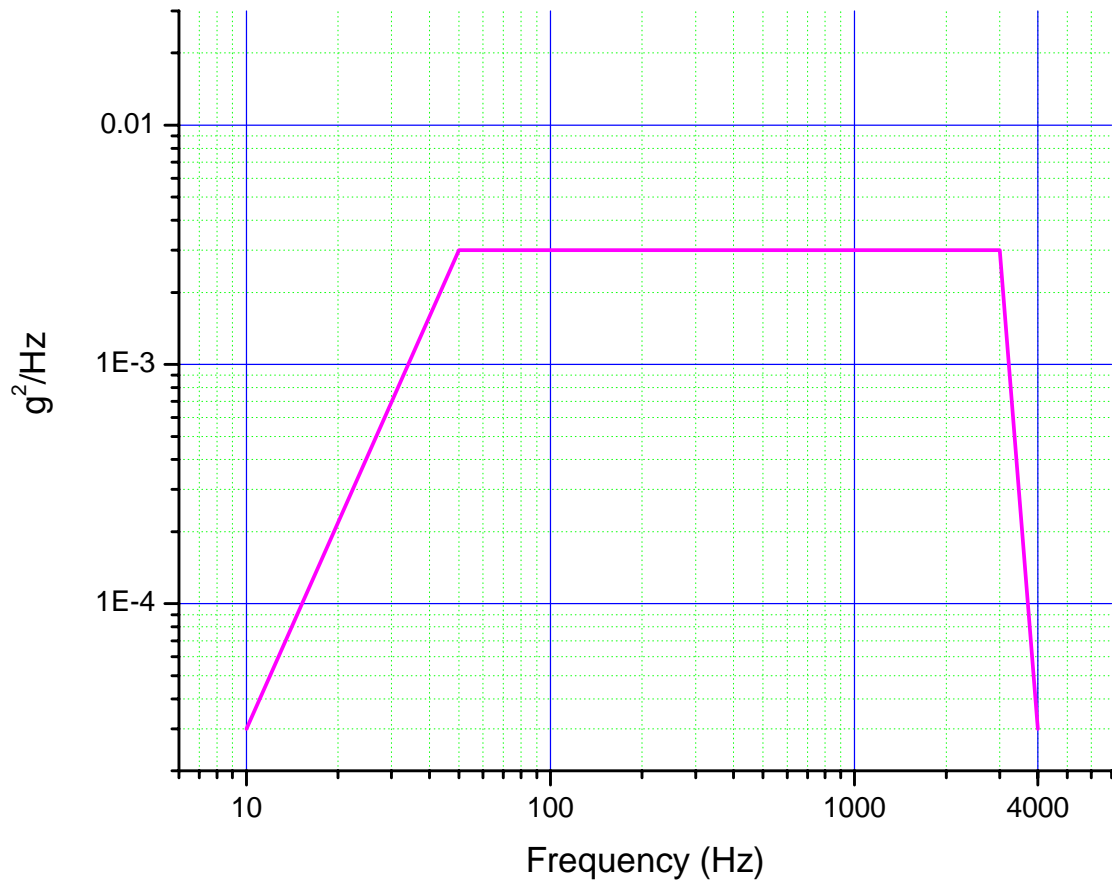


Figure 5: Typical Random Vibration Profile

*Individual tests were scaled to result in an overall g-level*

### 3.0 Presentation of Results

The outputs of the IMUs were analyzed by calculating the 1 sigma noise while in various vibration states. The deviation was normalized relative to the static 1 sigma noise levels for each device for ease of comparing the MEMSense performance gyros versus the IMU with low cost gyros. In all plots the low cost MEMS gyros were contained in serial numbers 202 and 203 (SN202 & SN203) while the performance gyros were in SN40.

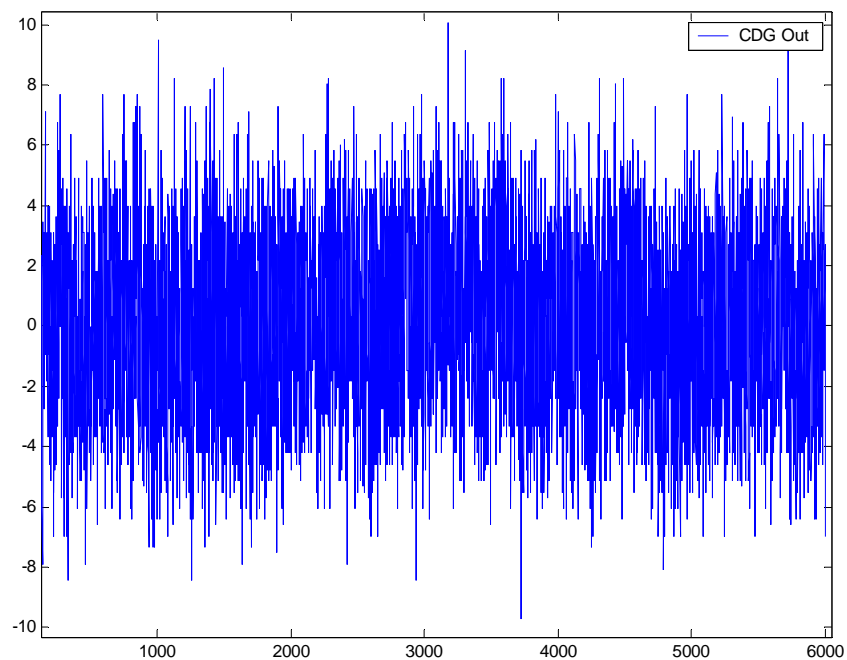


Figure 6: Raw Gyro Data, Output ( $^{\circ}/s$ ) vs. Sample Point

During the testing trials, the random vibration profile (Figure 5) was rescaled as appropriate to produce the desired RMS g-level. A plot was then made of the gyroscope output versus increasing vibration level. A plot such as the following (Figure 7) was produced after normalizing to the baseline noise.

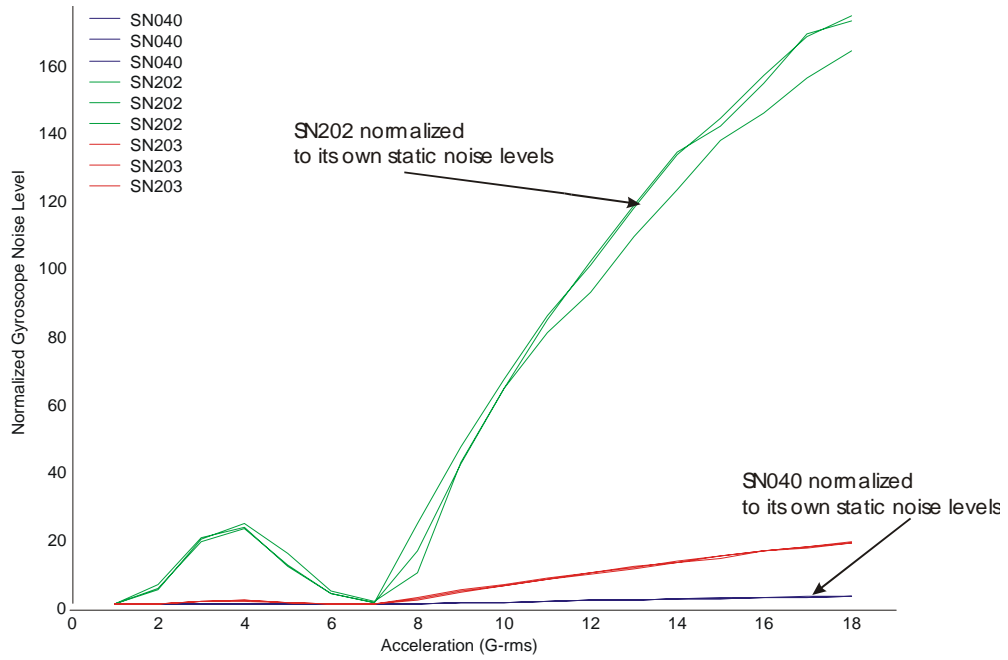


Figure 7: Analysis of IMUs Outputs

## 4.0 Results of Random Vibration Testing

### 4.1 MEMSense IMU (SN040) Baseline

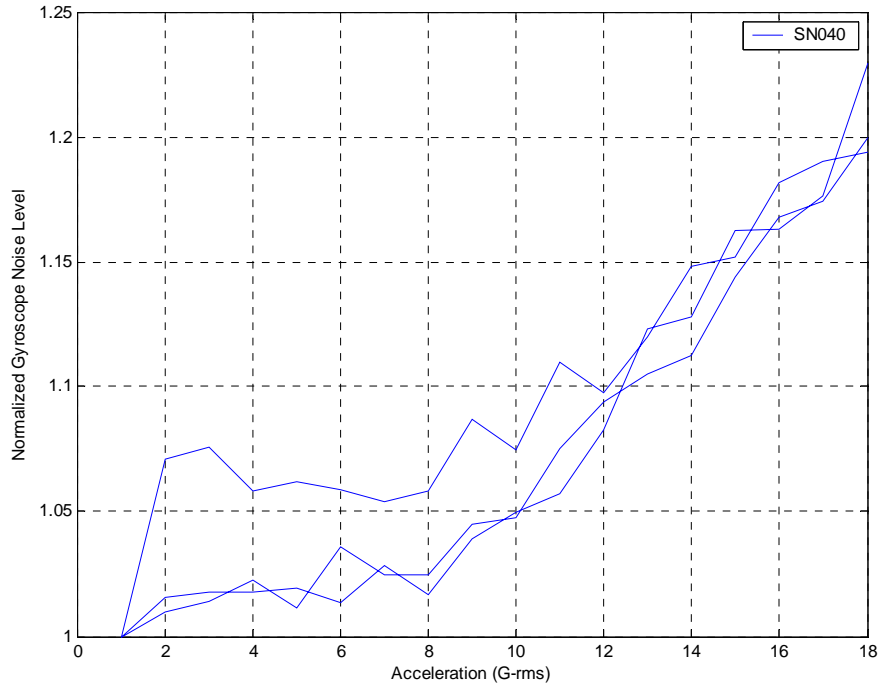


Figure 8: MEMSense IMU SN040 X-Gyro, X-Test

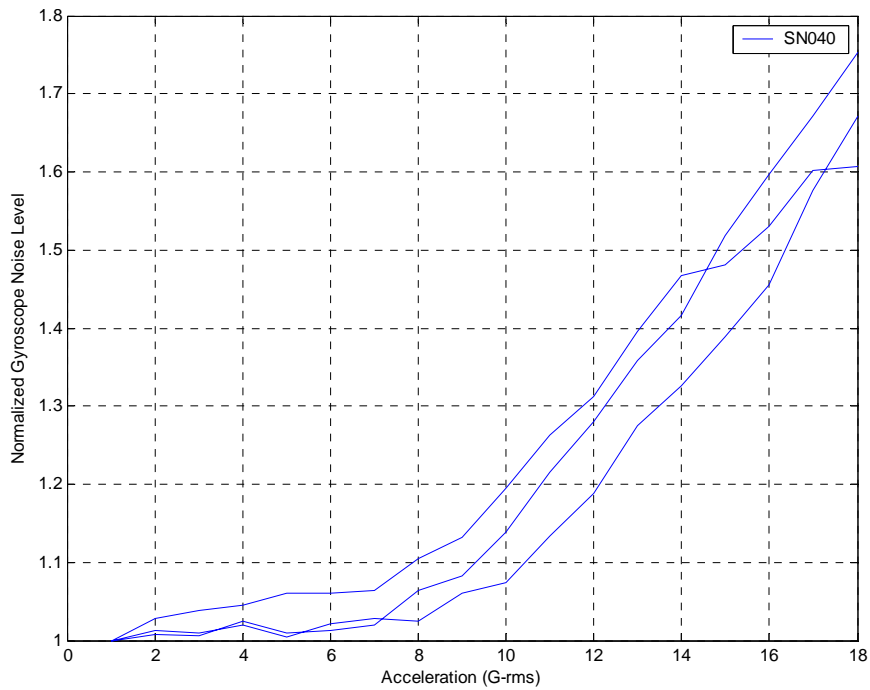


Figure 9: MEMSense IMU SN040 X-Gyro, Y-Test

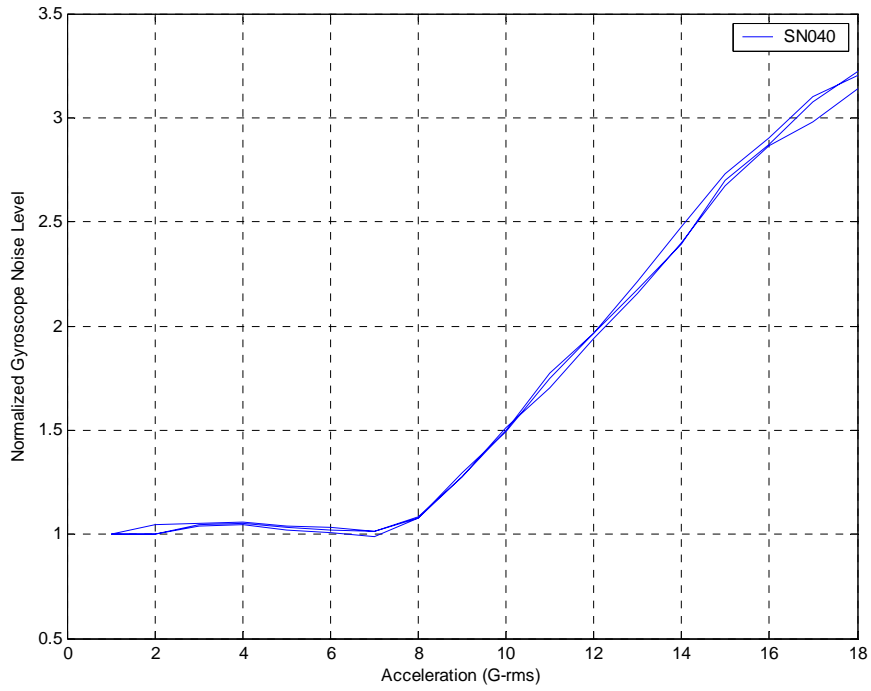


Figure 10: MEMSense IMU SN040 X-Gyro, Z-Test

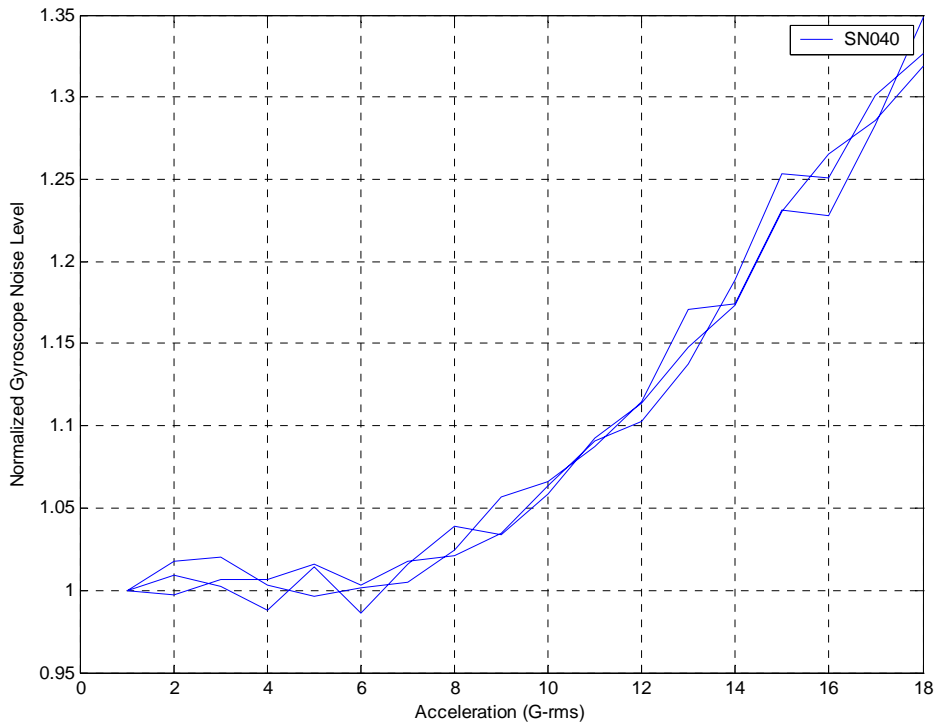


Figure 11: MEMSense IMU SN040 Y-Gyro, X-Test

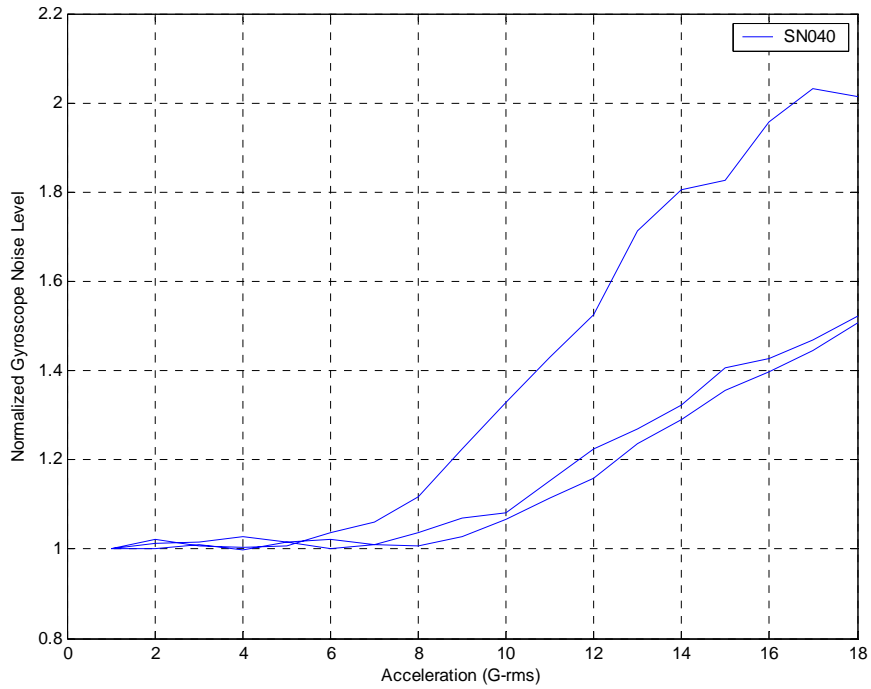


Figure 12: MEMSense IMU SN040 Y-Gyro, Y-Test

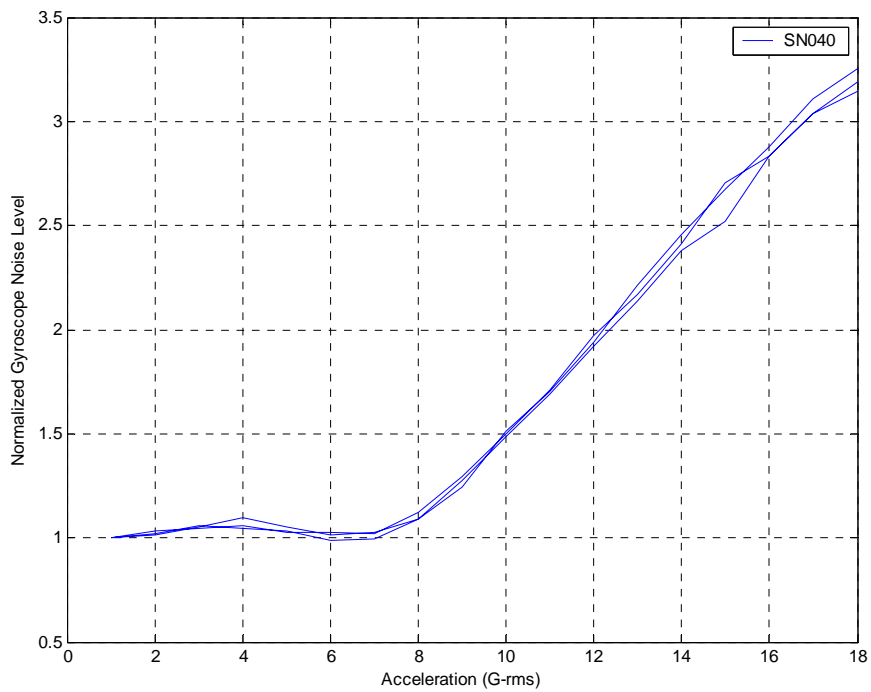


Figure 13: MEMSense IMU SN040 Y-Gyro, Z-Test

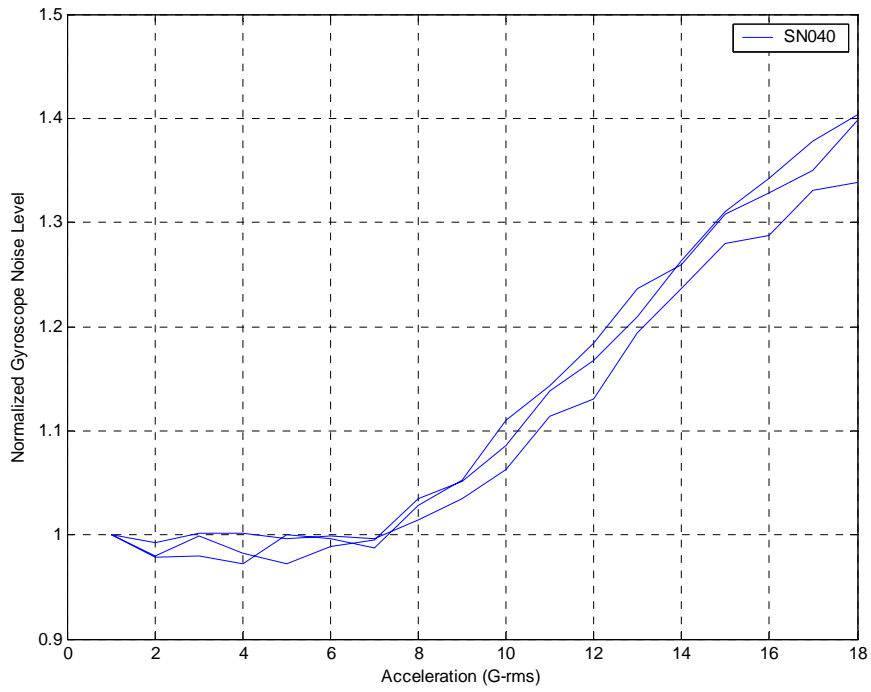


Figure 14: MEMSense IMU SN040 Z-Gyro, X-Test

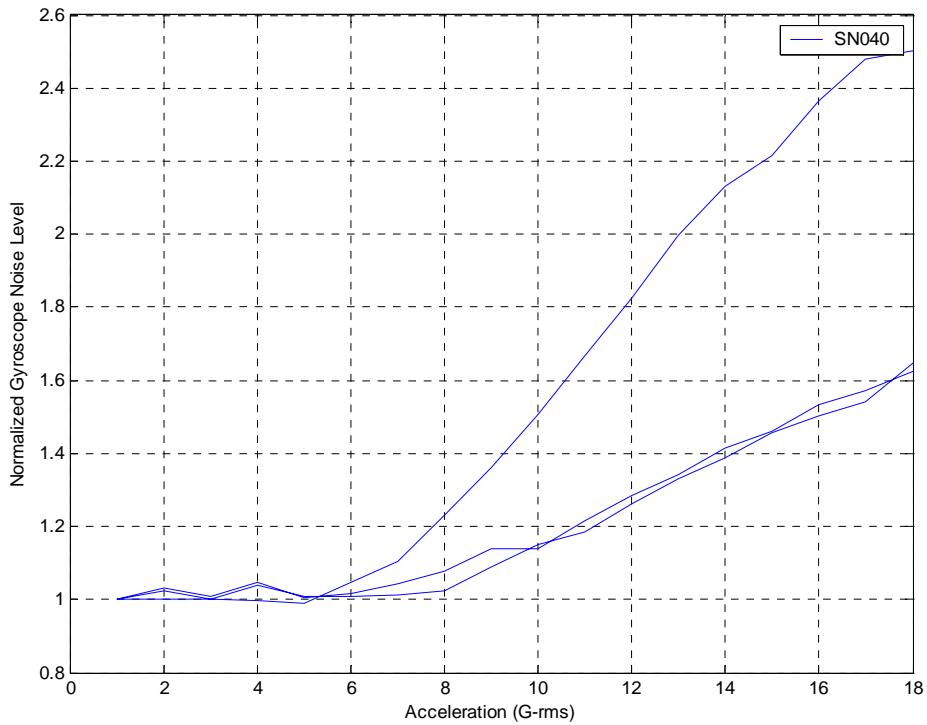


Figure 15: MEMSense IMU SN040 Z-Gyro, Y-Test

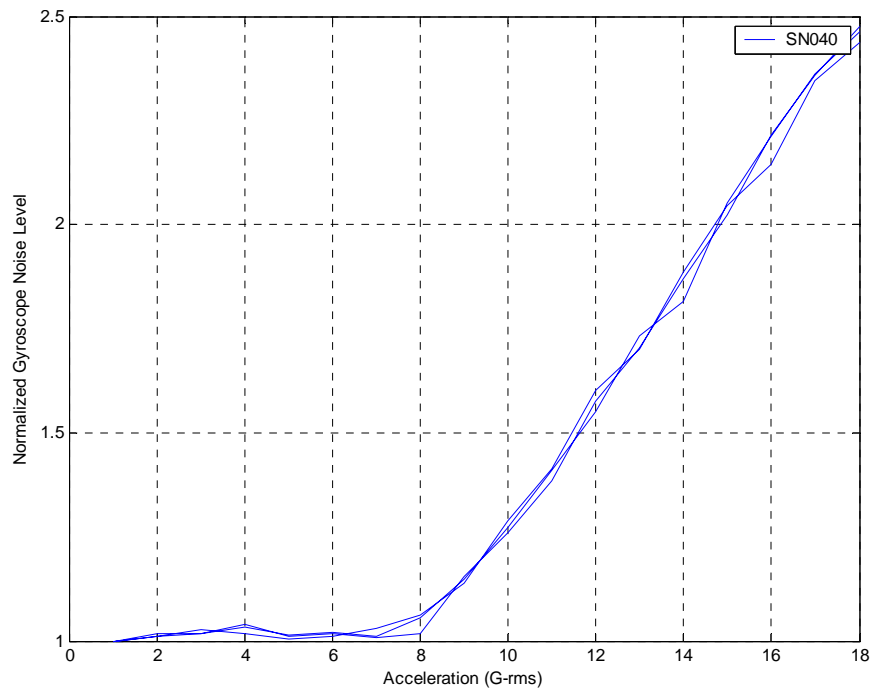


Figure 16: MEMSense IMU SN040 Z-Gyro, Z-Test

## 4.2 Comparison of MEMSense IMU (SN040) to Low Cost IMUs(SN202 & SN203)

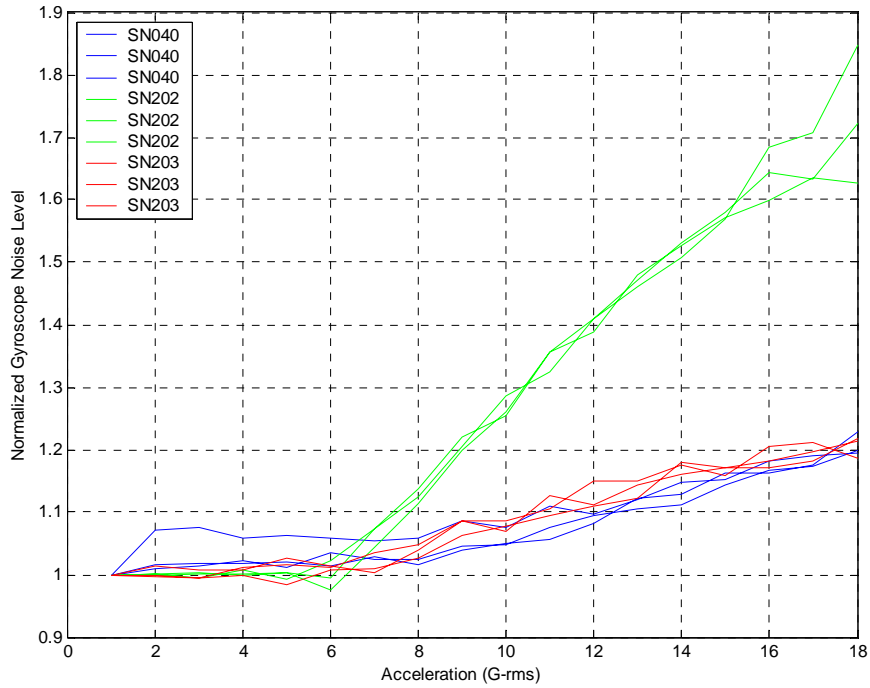


Figure 17: X-Gyroscope, X-Axis Vibration

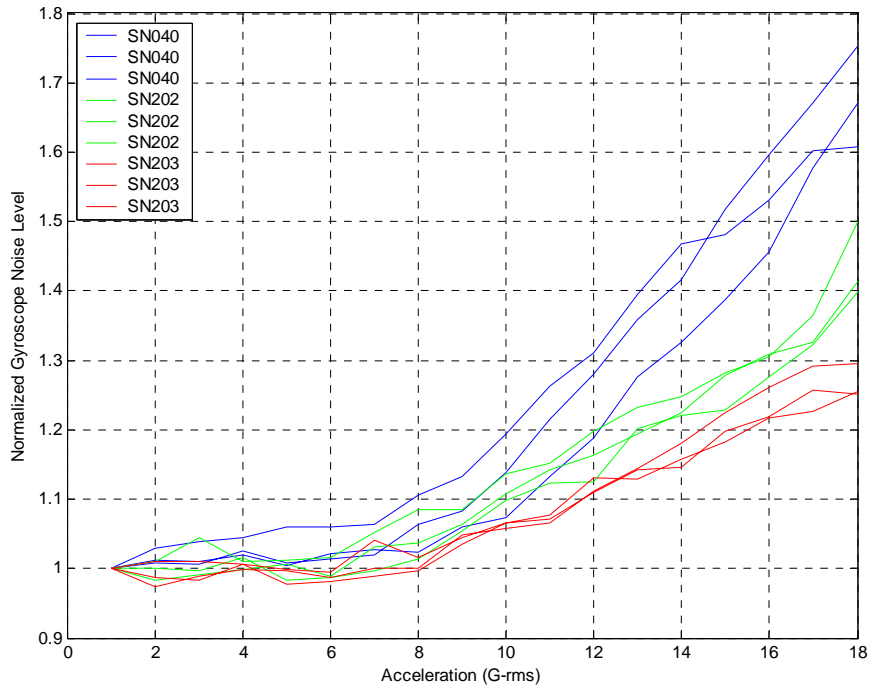


Figure 18: X-Gyroscope, Y-Axis Vibration

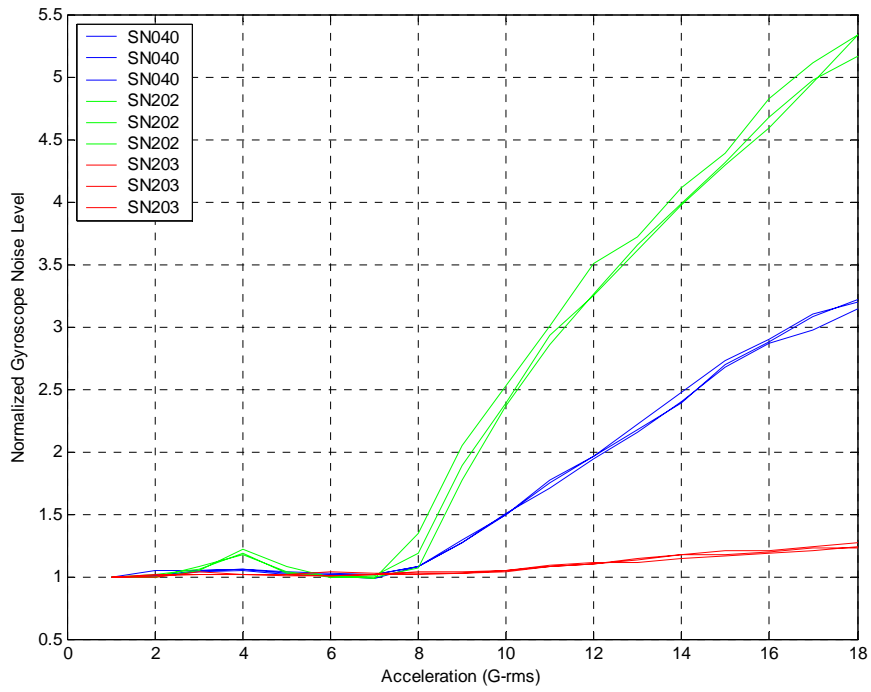


Figure 19: X-Gyroscope, Z-Axis Vibration

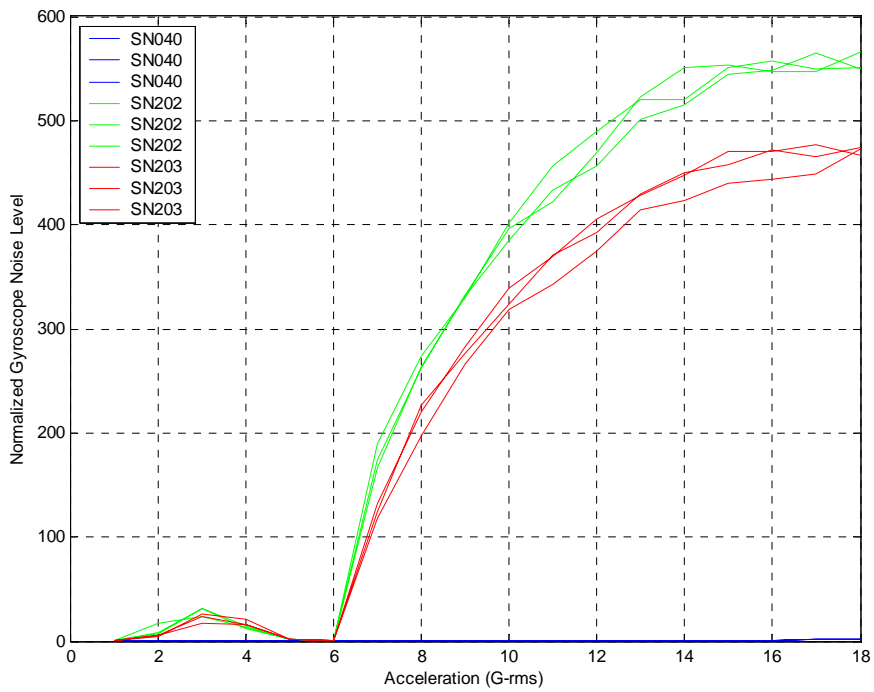


Figure 20: Y-Gyroscope, X-Axis Vibration

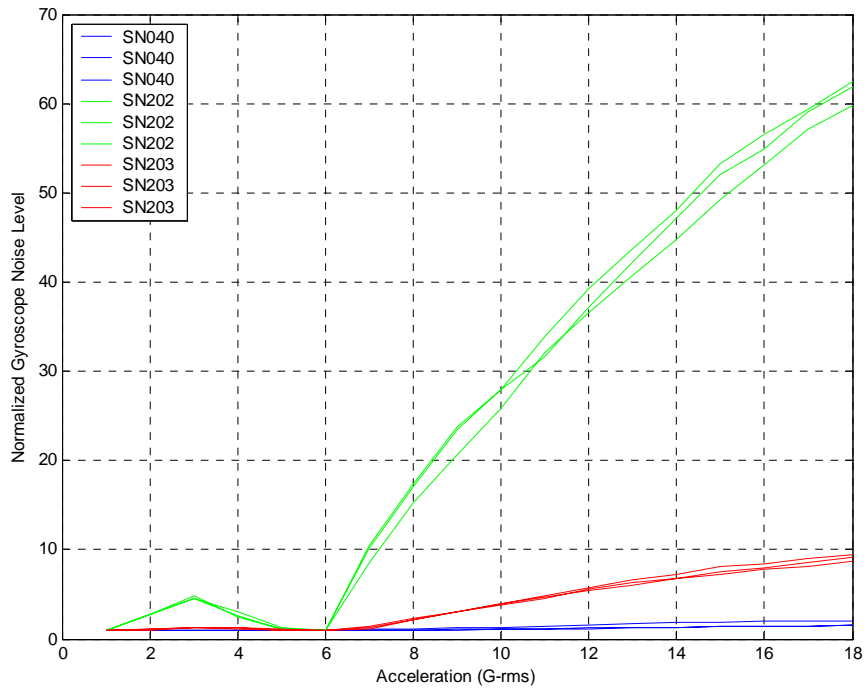


Figure 21: Y-Gyroscope, Y-Axis Vibration

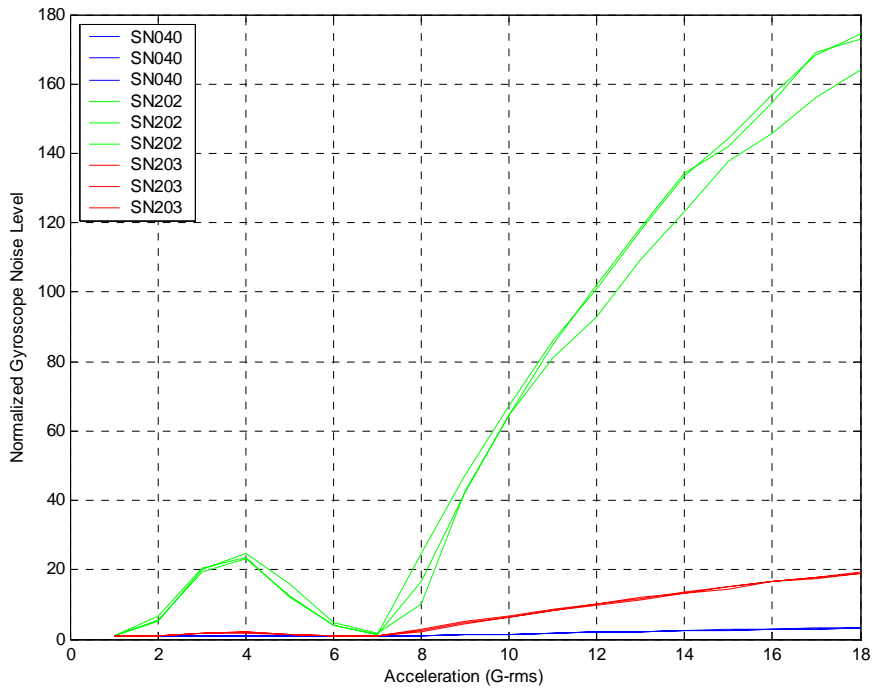
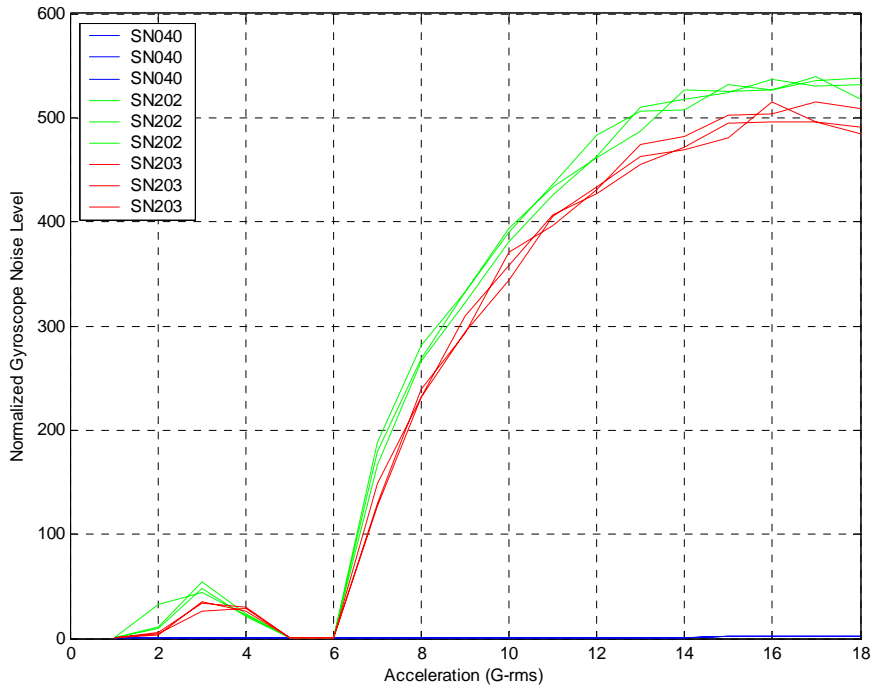
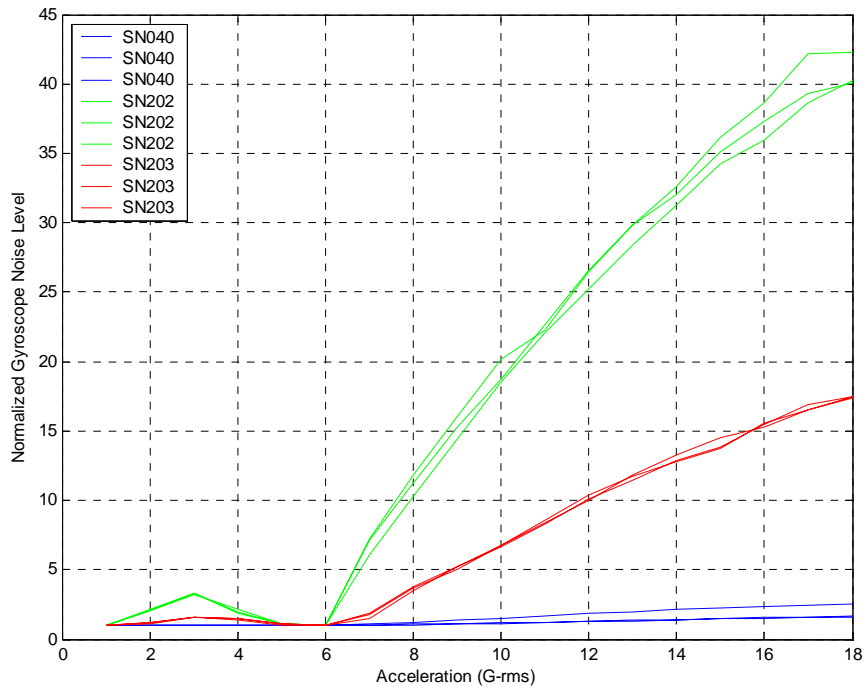


Figure 22: Y-Gyroscope, Z-Axis Vibration



**Figure 23: Z-Gyroscope, X-Axis Vibration**



**Figure 24: Z-Gyroscope, Y-Axis Vibration**

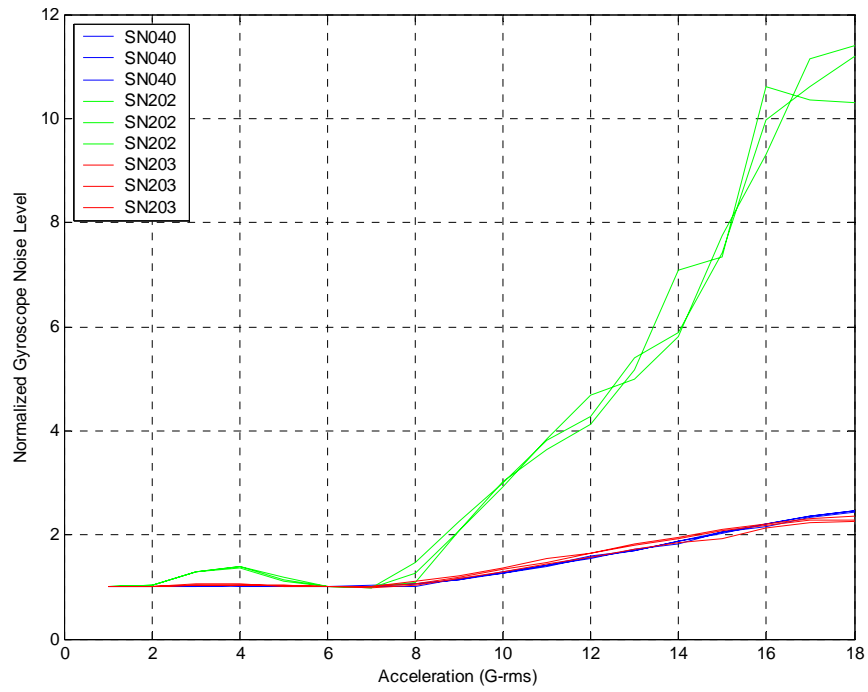


**Figure 25: Z-Gyroscope, Z-Axis Vibration**

## 5.0 Sine Sweep Results

A set of sine sweep tests were performed with frequencies ranging from 40Hz to 4 kHz. Each axis of the IMU containing low cost gyroscopes was tested and the gyro output was plotted vs. frequency. Some significant increases in noise were observed and the more notable instances have been marked as appropriate in the following plots. An individual noise event is characterized below by a multiplicative factor derived by taking the peak noise value and normalizing it to the 1-sigma noise level.

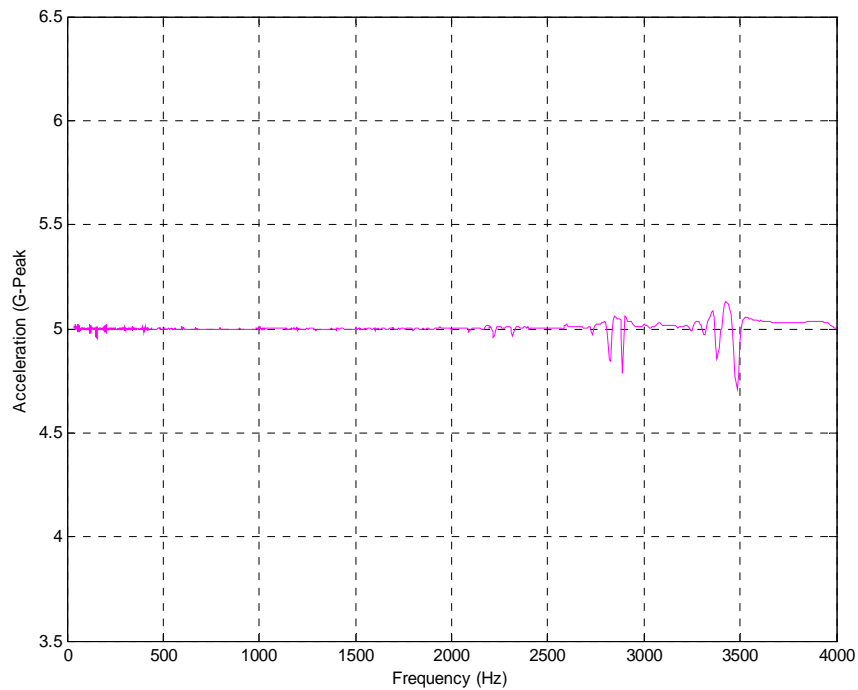


**Figure 26: Sine Input, 5G Sine Sweep**

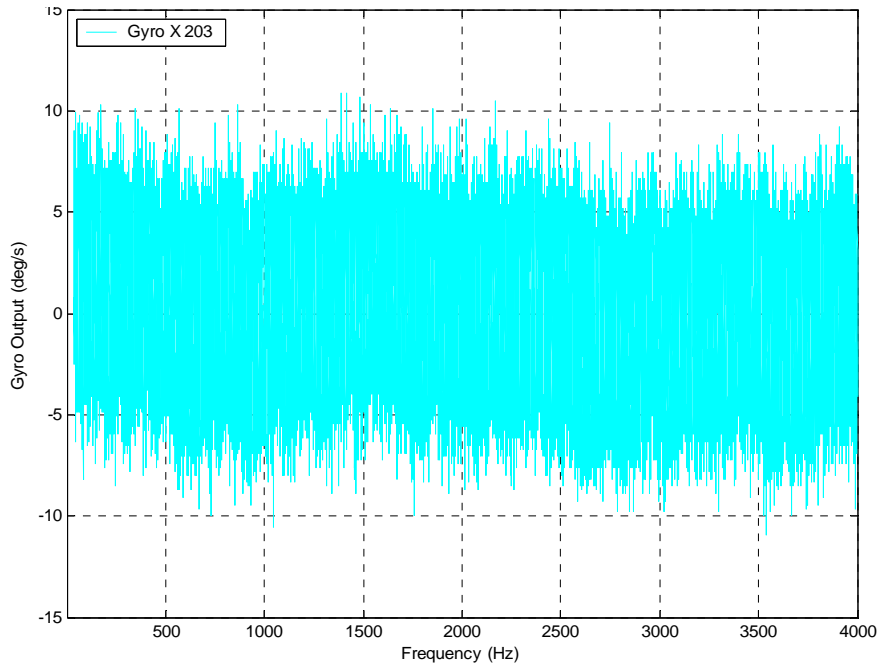


**Figure 27: IMU Sine Sweep Testing X-Gyro, X Axis**

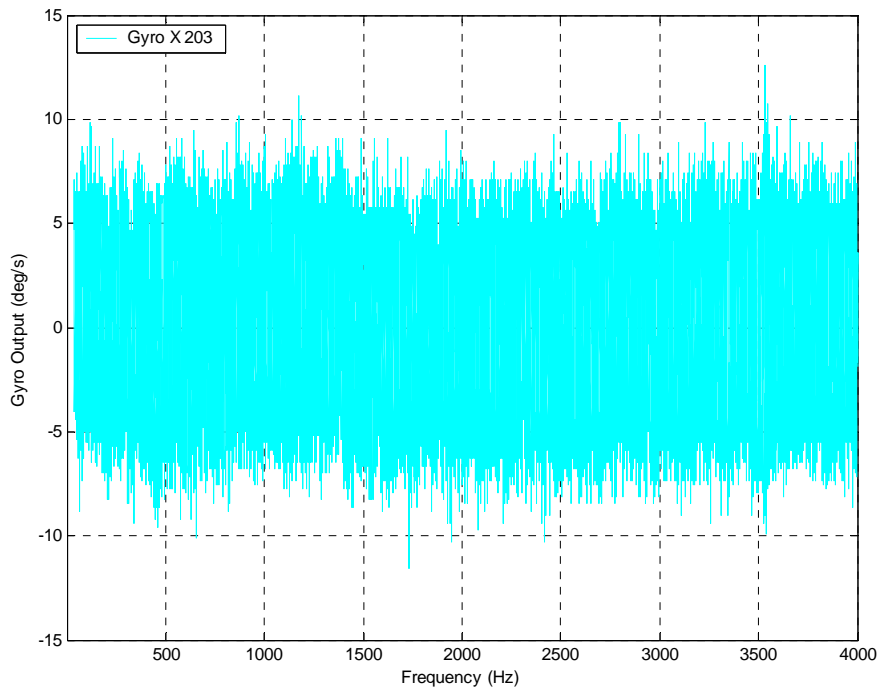


**Figure 28: IMU Sine Sweep Testing X-Gyro, Y Axis**

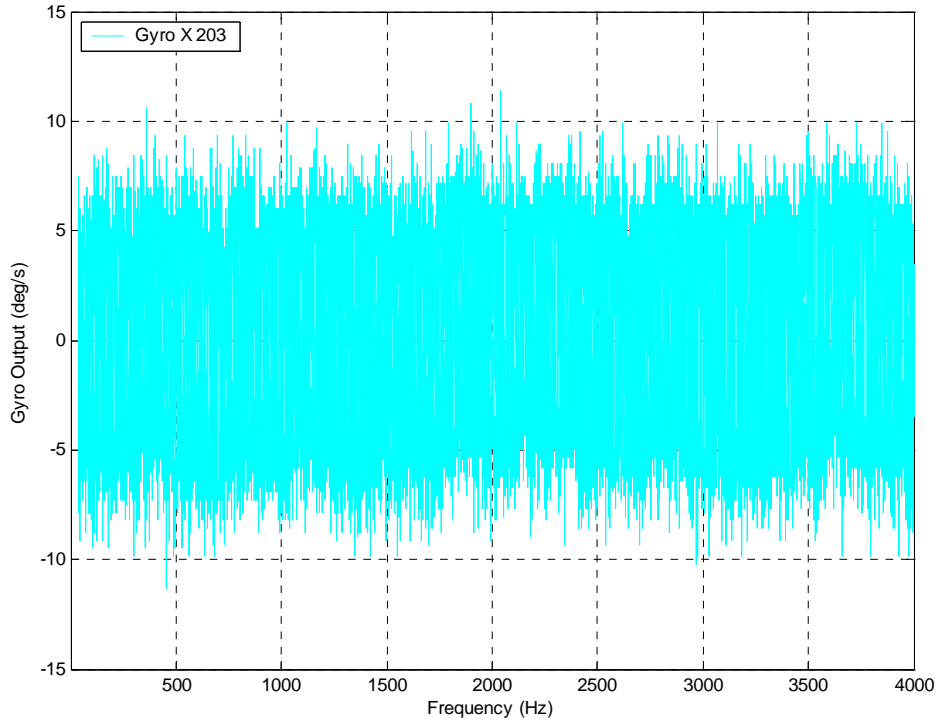


**Figure 29: IMU Sine Sweep Testing X-Gyro, Z Axis**

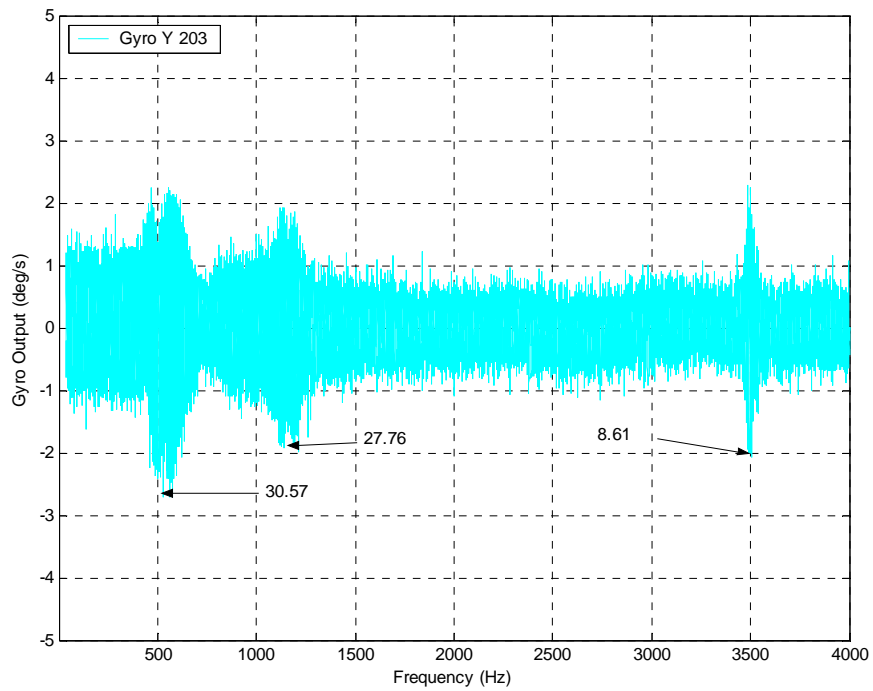


**Figure 30: IMU Sine Sweep Testing Y-Gyro, X Axis**

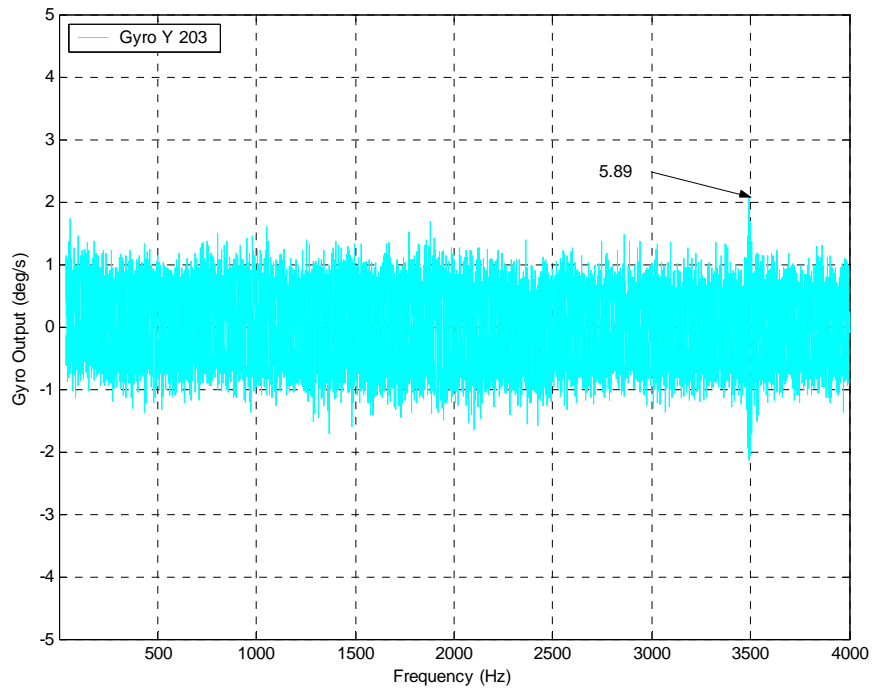


**Figure 31: IMU Sine Sweep Testing Y-Gyro, Y Axis**

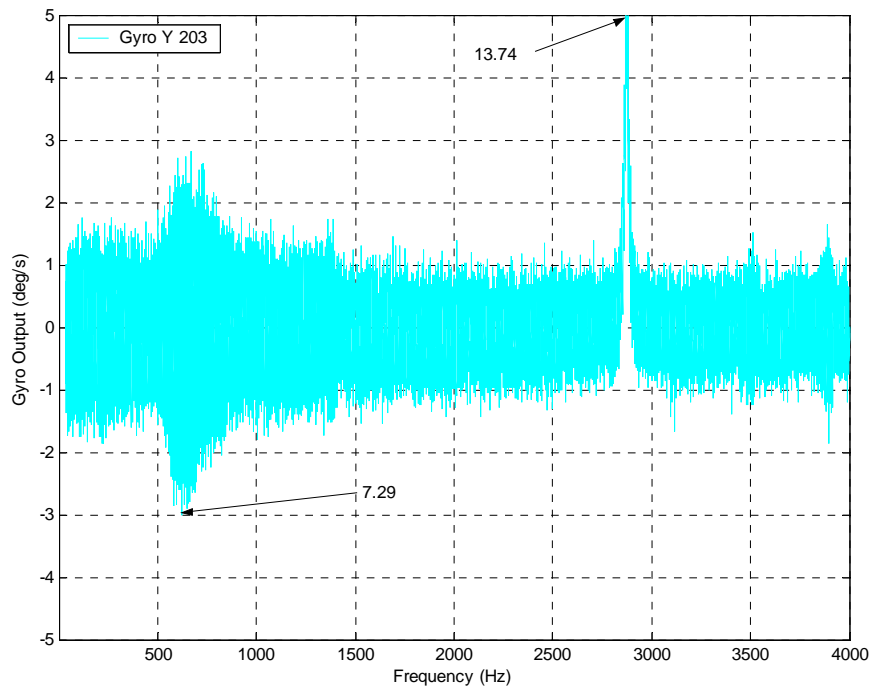


**Figure 32: IMU Sine Sweep Testing Y-Gyro, Z Axis**

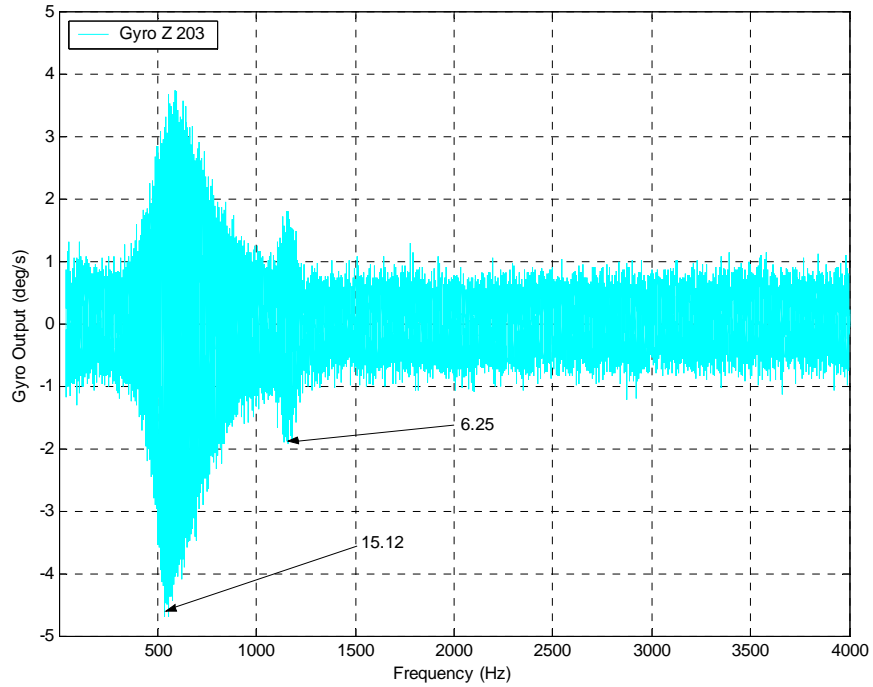


**Figure 33: IMU Sine Sweep Testing Z-Gyro, X Axis**

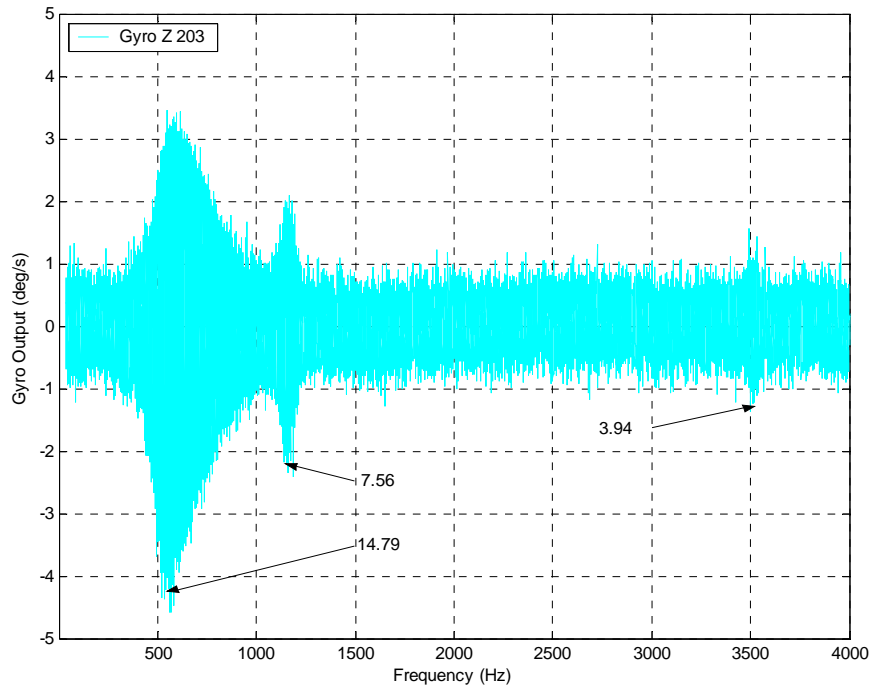


**Figure 34: IMU Sine Sweep Testing Z-Gyro, Y Axis**

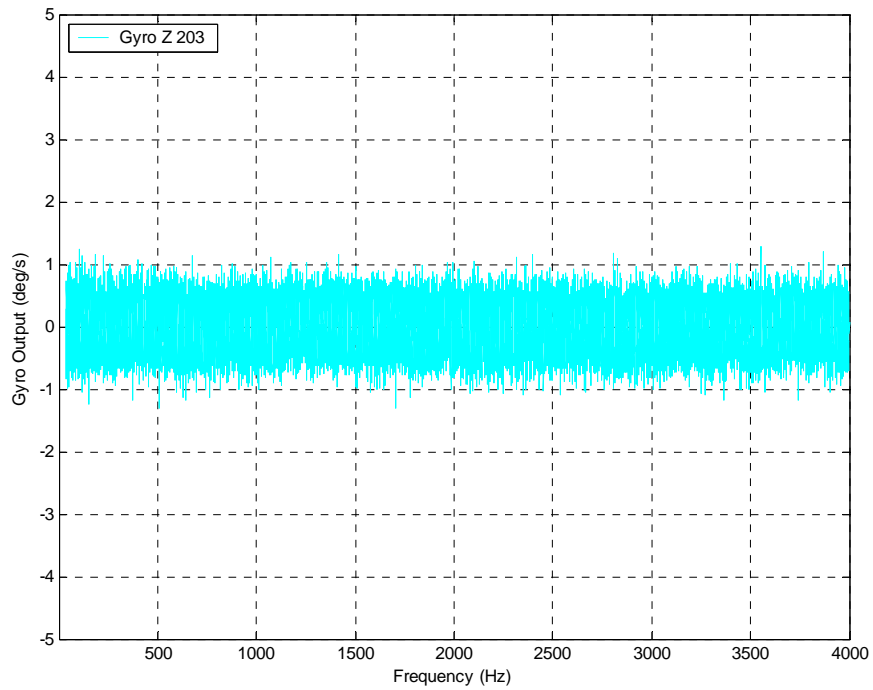


**Figure 35: IMU Sine Sweep Testing Z-Gyro, Z Axis**

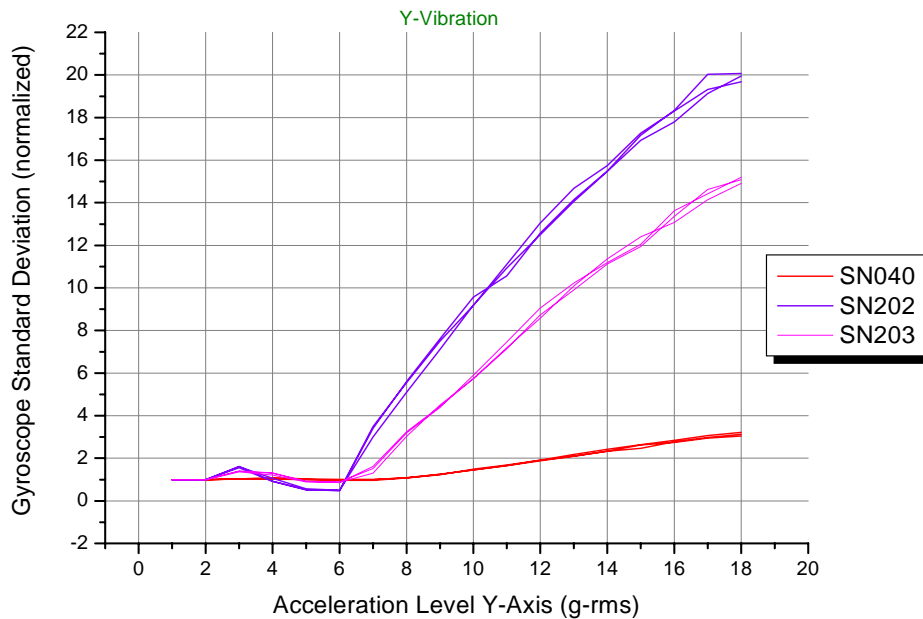


**Figure 36: Z Gyro Output - Acceleration rate sensitivity appears at 3G level**

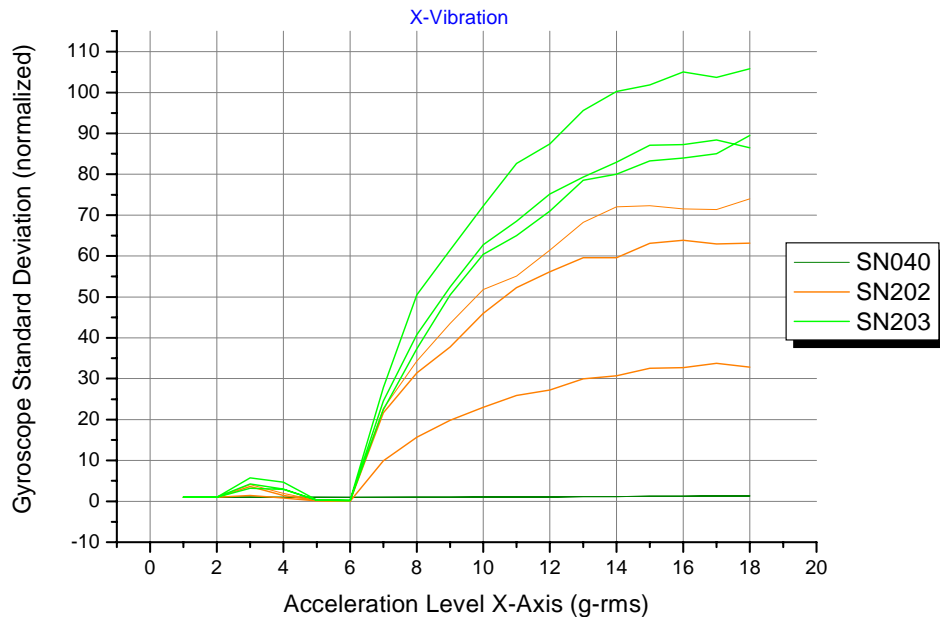


**Figure 37: Y Gyro Output Acceleration noise threshold appears at 6G level**

Figures 36 and 37 show the severe increase in noise levels due to vibration in the IMU containing the low cost gyroscopes. When acceleration levels go beyond the 6g level, noise increases non-linearly having reached the limits of sensitivity and then surpass those limits to saturation. The acceleration threshold appears at approximately 6g-rms in this instance (Fig. 36) and the nonlinear effects are visible in Fig. 37.

A notable increase in noise was observed at the 3g level in most axes of the low cost gyroscope. The cause of this increase may be related to sensitivity to linear acceleration rate (jerk). The MEMSense IMU's gyro has never displayed such behavior at any random acceleration level while testing to these vibration specifications.

## 6.0 Summary

The results have been presented in the form of noise levels plotted vs. acceleration input level. A typical random vibration profile was run on an electrodynamic shaker and scaled to fulfill an overall vibration acceleration level ranging from 1g-rms to 18g-rms. The gyroscope outputs were characterized via the calculation of the standard deviation of a sample of data collected during vibration and normalized with its own idle noise levels. This normalization was carried out to compare low cost triaxial gyros used in IMUs with gyros used in MEMSense IMUs.

The IMUs containing the low cost MEMS gyros exhibited high cross-axis sensitivity to random vibration profiles. The results indicate that the low cost MEMS gyros may have poor vibration rejection characteristics. Gyro noise reached high levels in the IMUs containing low cost gyros during random vibration conditions. The effects were especially observable in off-axis vibration modes. The effect was present in almost all trials and with only a few exceptions, the noise would preclude the use of these sensors for inertial measurement in high vibration environments. The resolution of solid-body motion is problematic even at relatively low acceleration levels (2-6g-rms) with frequency content between 100 Hz and 4 kHz.